

Measurements and simulations for CBM TRD.

Dmitry Blau

Institute of Natural Science and Ecology at Russian Research
Center "Kurchatov Institute"
blau@vskur4.mbslab.kiae.ru
Marshala Novikova str., 2, 59.
Moscow, Russia
7-095-1963814



In the framework of CBM experiment the geometry of Transition Radiation Detector was designed. Its performance was investigated and comparison with previous one (simplified) was carried out.

1 Introduction

The exploration of the phase diagram of strongly interacting matter is one of the most challenging fields of modern physics. Of particular interest is the transition from hadronic to partonic degrees of freedom which is expected to occur at high temperatures and/or high baryon densities. QGP phase played an important role in the early universe and possibly exist in the core of neutron stars. Of course, the nuclear fireball produced in heavy ion collisions differs drastically from a neutron star in size, lifetime, temperature and isospin. Nevertheless, one can obtain experimental information on superdense strongly interacting matter which is of relevance for astrophysics. Some of the most fascinating features of strong interaction physics are still not quantitatively understood: the phenomenon of confinement (why are quarks not observed as individual particles?) and the origin of the mass of hadrons (why is a hadron - that is composed of light quarks - much heavier than the sum of the masses of its constituents?).

The planned SIS 300 synchrotron at the future FAIR facility covers an energy range of up to 45 AGeV for nuclei with $A=2Z$, and, hence, is well suited to explore the high baryon density region of the QCD phase diagram. The research programme to be performed with the proposed Compressed Baryonic Matter (CBM) experiment includes a comprehensive investigation of the relevant hadronic observables, and is focused on systematic measurements

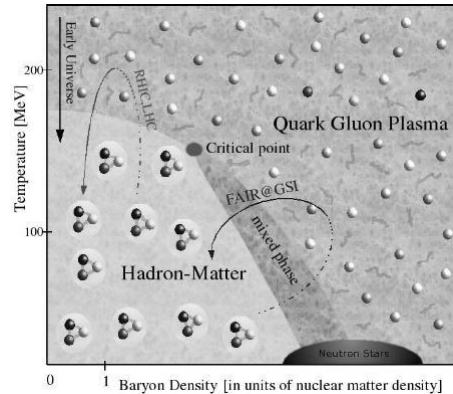


Fig. 1: *The phase diagram of strongly interacting matter plotted as a function of temperature and baryochemical potential.*

of diagnostic probes which have not been measured before in this energy range: the dileptonic decay of low-mass vector mesons and hadrons containing charmed quarks.

The detector layout comprises a high resolution Silicon Tracking System in a dipole magnetic field for particle momentum and vertex determination, Ring Imaging Cherenkov Detectors and Transition Radiation Detectors for the identification of electrons, an array of Resistive Plate Chambers for hadron identification via TOF measurements, and an electromagnetic calorimeter for the identification of electrons, photons and muons.

Here we will discuss the CBM Transition

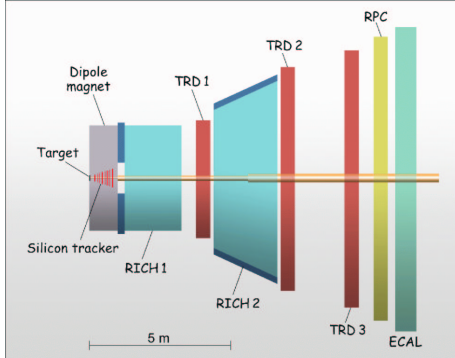


Fig. 2: Proposed scheme of CBM subdetectors

Radiation Detector (TRD) performance. The TRD will provide electron identification and tracking of all charged particles. It has to provide, in conjunction with the RICH detector and the electromagnetic calorimeter, sufficient electron identification capability for the measurements of charmonium and of low-mass vector mesons. In order to fulfill these tasks, in the context of the high rates and high particle multiplicities in CBM, a careful optimisation of the detector is required.

In order to archive the necessary pion rejection it is currently anticipated to build nine layers of TRDs. There will be three stations of detectors at distances of 4 m, 6 m, and 8 m from the target. A detailed study of the tracking performance in combination with all the CBM subdetectors is needed for a final decision on such a segmentation, as well as for the final requirements on position resolution within each of the planes. The total thickness of the detector in terms of radiation length has to be kept as small as possible to minimise multiple scattering and conversions. The gas mixture of the readout detectors has to be based on Xe, to maximize the absorption of transition radiation (TR) produced by the radiator. Because of the high rate environment expected in the CBM experiment, a fast readout detector has to be used.

2 Physics performance

Transition Radiation (TR) is produced when ultra relativistic particles cross the boundary between two media with different dielectric constants. TR is X-rays of about 10 KeV.

This phenomenon is used in the CBM experiment to separate pions from electrons, since pions do not produce any TR. This is due to their large mass because the intensity of TR is proportional to Lorentz factor γ ($\gamma \simeq E/m$). The emission angle of TR is concentrated in a narrow cone of an angle $\theta \simeq 1/\gamma$.

Electrons generated by gas ionization and by absorption of TR photons on the track as well as primary electrons, which come from the interaction of the charged particle with the atoms of gas, drift towards the anode wires where they trigger avalanches due to the ionization of atoms.

The electrons travel to the anode while the positive ions give the signal on the pad plane. As a signature to identify electrons we can use the larger ionization energy loss of electrons as compared with pions and also the energy deposit due to transition radiation.

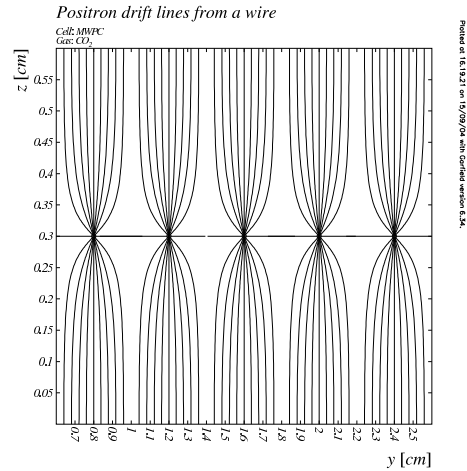


Fig. 3: Layout of one chamber.

For momenta of several GeV/c, due to the relativistic rise of the pions, the separation between the pions and the electrons based on ionization only is reduced as a function of momentum based on the fact that the TR of pions is negligible, the contribution of TR of the electrons can achieve a good electron/pion identification.

Computation of the transition radiation spectra in the radiator is done with a simplified formula:

$$\frac{dW}{d\omega} = \frac{4\alpha}{\sigma(\kappa + 1)} (1 - \exp(-N_f \sigma)) \sum_n \Theta_n \times \left(\frac{1}{\rho_1 + \Theta_n} - \frac{1}{\rho_2 + \Theta_n} \right)^2 [1 - \cos(\rho_1 + \Theta_n)] \quad (1)$$

where:

$$\begin{aligned} \rho_i &= \frac{\omega d_1}{2c} (\gamma^{-2} + \xi_i^2), \\ \kappa &= d_2/d_1, \\ \Theta_n &= \frac{2\pi n - (\rho_1 + \kappa \rho_2)}{1 + \kappa} > 0, \\ \xi &= \omega_{plasma}/\omega. \end{aligned} \quad (2)$$

d_1 , d_2 are the foil thickness and gap width, respectively, and N_f is the number of foils. ω_{plasma} is the plasma frequency of the material, ω if the frequency of the emitted photon, σ is the absorption coefficient of the radiation in one (foil + gap) layer of the radiator.

3 Detector geometry

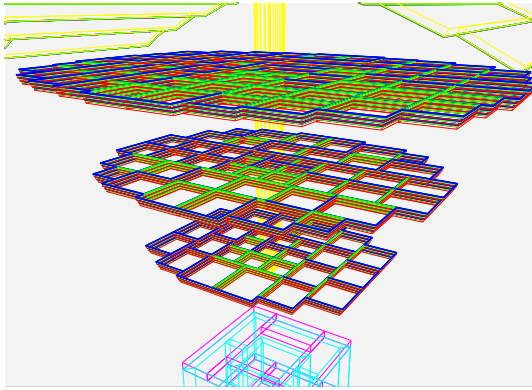


Fig. 4: Three TRD stations in 3D view of the CBM geometry.

One of the most important tasks in the preliminary investigation of the TRD detector is to choose the right geometry of it. The geometry was produced by standalone C++ based code. The three stations, which are shown on the Fig.4, differ from each other in size and segmentation. The geometry was chosen in order to cover an ellipse of 30 degrees to 25 degrees from

the target (it is about $4.8 \times 4.0 m^2$ for the first layer of the first station). All layers presented on the Fig. 5 consist of 4 different chambers (some of them are rotated by 90°).

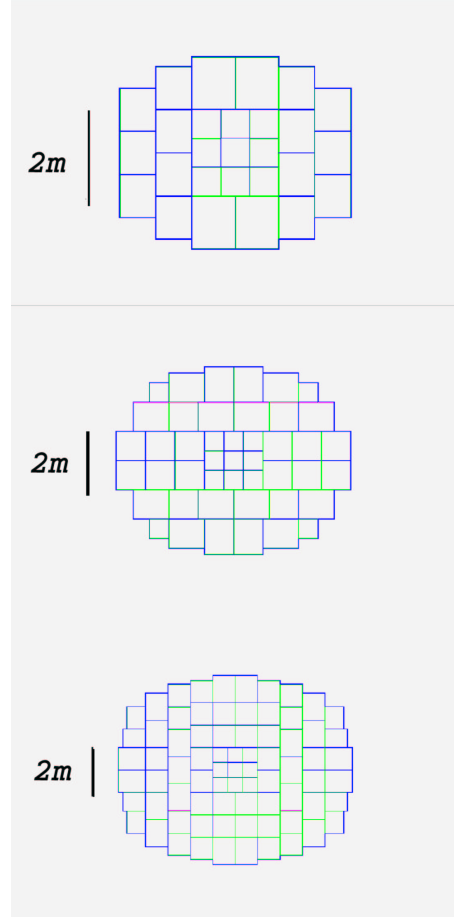


Fig. 5: Front view of geometry of the TRD stations.

Next layers of stations (second and third in this geometry) are simply rescaled from first ones in order to not allow shadows from frames to be in the active volumes. Therefore the total number of different types of chambers is 12. The size of the biggest chamber is $905 \times 1100 mm^2$, which is a practical size for construction. The total number of chambers in all layers of all stations is 432.

The front view of the stations' geometry that is in use at the moment can be seen on the Fig. 5. One chamber consists of radiator, gas, pad-plane, mylar, electronics and gap layers. Radiator thickness is 3 cm and its material is polypropylene. Readout chamber consists of 6 mm thick gas layer filled with Xe/CO_2 (85/15)

mixture, padplane $50 \mu\text{m}$ thick, mylar foil 2 mm thick, electronics layer of 0.1 mm thickness. The rest (21.4 mm) is empty. Each chamber is rounded by a frame of $1 \times 1\text{cm}^2$ dimensions made of carbon.

4 Simulations and results

Introduction of new geometry in the cbmroot2 [5] framework was carried out and the preliminary comparison of the main characteristics of two types of TRD geometries was done. First type of TRD geometry consists of simple layers (without segmentation to chambers). Second type is presented in the section 3. On the following plots these types are called old and new geometries, respectively. The comparison was done in means of Monte Carlo points.

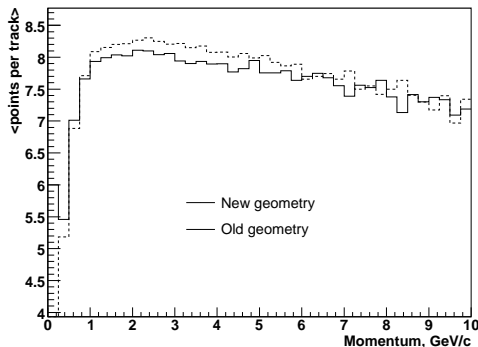


Fig. 6: Mean value of TRD points per track for primary particles (producing more than 4 out of 7 points in STS).

In the comparison of the mean value of TRD points of primary particles per track depending on momentum of particles one can see that in the range from 1 till 10 GeV/c there is almost constant behaviour at the value of 8 TRD points per track with a slight slope down into the range of high momentum, which is probably caused by too large beam pipe hole in the first station and therefore not matching the acceptance of the Silicon Tracking Station (STS). For momenta higher than 6 GeV/c there are some fluctuations in the values of bins caused by too small statistics. Histograms corresponding to new and old geometries are close to each other therefore we can conclude that segmentation of TRD planes and effect of carbon frames

in particular have small significance on this characteristic of the detector.

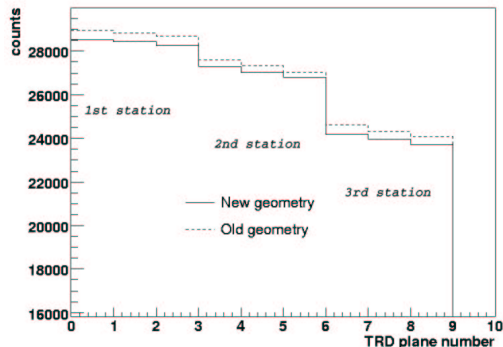


Fig. 7: Number of points produced in each TRD plane by primary particles. $3 \times 3\text{m}^2$ square cut without $70 \times 70\text{cm}^2$ hole was applied.

Number of points created by primary particles per plane is presented in the Fig. 7. We have applied a cut on the X and Y position of the point to cancel the effect of different angular coverages of the new and old geometry caused by complicated shape of the new geometry and due to the fact that the old geometry has an increasing size of the beam pipe hole.

Decreasing of TRD points in the second and third station is caused by smaller angular coverage of the equal in the area parts of the detector. The difference in the values of new and old geometries is approximately 2%. This difference is mainly due to the introduction of the frames (inactive volume) in the new geometry.

5 Conclusion

Differences in detector performance for new and old geometries are relatively small, but it is clear that the more precise and detailed investigation of the new geometry and comparison with previous one is still needed (in particular using the global tracking). Moreover, the new geometry is still in the developing stage and will be modified and improved.

Acknowledgments

I would like to thank my tutor Anton Andronic for his help and support, Matus Kalisky who worked with me and explain me everthing, V.G. Orlov, I.M. Pavlichenkov, S.T. Belyaev, V. Volkov from Kurchatov Institute who helped me to attend to the Summer Student Program at GSI.

References

- [1] The CBM collaboration, *Letter of Intent for the Compressed Barionic Matter Experiment at the Future Accelerator Facility in Darmstadt*, Darmstadt, January 2004.
- [2] The CBM collaboration, *Technical Status Report for the Compressed Baryonic Matter Experiment*, Darmstadt, February 2005
- [3] A. Andronic, *Transition Radiation Detector study*, GSI, Darmstadt.
- [4] Christos Tagridis, *Test of Prototype Detectors for ALICE TRD*, Summer Student Reports 2004.
- [5] D. Bertini, M. Al-Turany, *CBM simulation software*,
www-linux.gsi.de/~gsisim/cbm.html